

Highlights of Spanish Astrophysics VIII, Proceedings of the XI Scientific Meeting of the Spanish Astronomical Society held on September 8 – 12, 2014, in Teruel, Spain. A. J. Cenarro, F. Figueras, C. Hernández-Monteagudo, J. Trujillo, and L. Valdivielso (eds.)

A photometric variability study of massive stars in Cygnus OB2

J. Salas¹, J. Maíz Apellániz², and R. H. Barbá³

¹ Agrupación Astronómica de Huesca, Spain

² Centro de Astrobiología, INTA-CSIC, Spain

³ Universidad de La Serena, Chile

Abstract

We have conducted a 1.5-year-long variability study of the stars in the Cygnus OB2 association, the region in the northern hemisphere with the highest density of optically visible massive stars. The survey was conducted using four pointings in the Johnson R and I bands with a 35 cm Meade LX200-ACF telescope equipped with a 3.2 Mpixel SBIG ST10-XME CCD camera and includes 300+ epochs in each filter. A total of 1425 objects were observed with limiting magnitudes of 15 in R and 14 in I . The photometry was calibrated using reference stars with existing $UBVJHK$ photometry. Bright stars have precisions better than 0.01 magnitudes, allowing us to detect 52 confirmed and 19 candidate variables, many of them massive stars without previous detections as variables. Variables are classified as eclipsing, pulsating, irregular/long period, and Be. We derive the phased light curves for the eclipsing binaries, with periods ranging from 1.3 to 8.5 days.

1 Survey description

We have conducted a one-and-a-half-year-long (25 June 2012 to 27 November 2013) variability study of Cygnus OB2 in the Johnson R_J and I_J bands (not Cousins) with Optec Inc. filters. We used a 35 cm Meade LX200-ACF telescope with an SBIG ST10-XME 3.2 Mpix. camera from a suburban location in Zaragoza, Spain, at an altitude of 260 m. We obtained over 300 epochs per filter in four $22.5' \times 15'$ fields (Figure 1). Our coverage extends to $R_J = 15$ and $I_J = 14$ (S/N limited), with 1425 objects, and there are only four saturated stars in the four fields: HD 195 988, Cyg OB2-5 A, Cyg OB2-8 A, and BD +40 4241 (Figure 1).

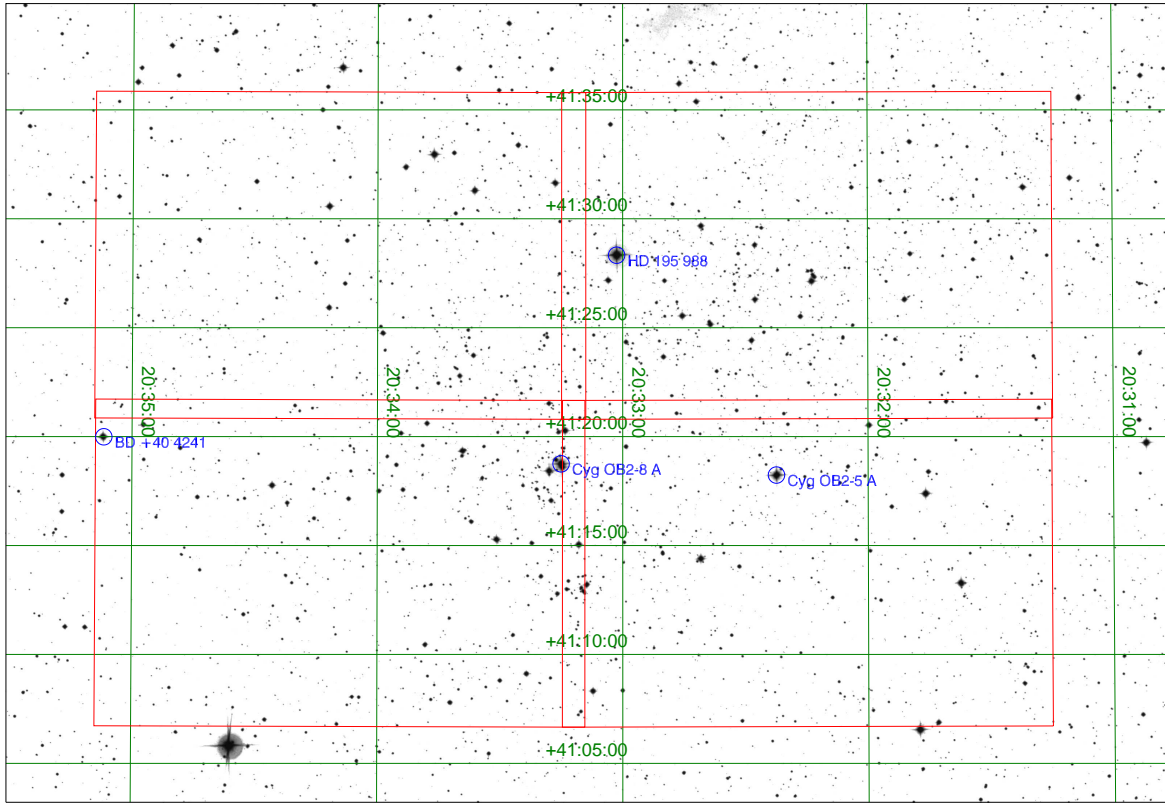


Figure 1: The four fields used in this work on a DSS2 Red image.

2 Why Cygnus OB2?

Cygnus OB2 is the best region to study O stars in the northern hemisphere for three reasons: (a) it is young and massive, including two O3 stars (the only cases with $\delta > 0$); (b) it has a well-populated IMF; and it is nearby (~ 1.7 kpc) but it has mid-to-high extinction ($A_V = 4\text{--}10$ mag). Note that Cygnus OB2 is an OB association, not a cluster (and it was born that way, Wright et al. 2014), so it is relatively extended in the sky. The spectral types for this work were obtained from the Galactic O-Star Catalog (Maíz Apellániz et al. (2004); Sota et al. 2008) and the Galactic O-Star Spectroscopic Survey (Maíz Apellániz et al. 2011).

3 Data taking and reduction

The observations were automated using CCD AutoPilot and MaxImDL / MaxPoint software. The image processing was done under Pyraf with additional Python packages and scripts. For the astrometric calibration we used <http://astrometry.net>. We performed aperture photometry with four different apertures. The selection among them was based on optimal S/N and minimal neighbor contamination on a case-by-case basis. The absolute

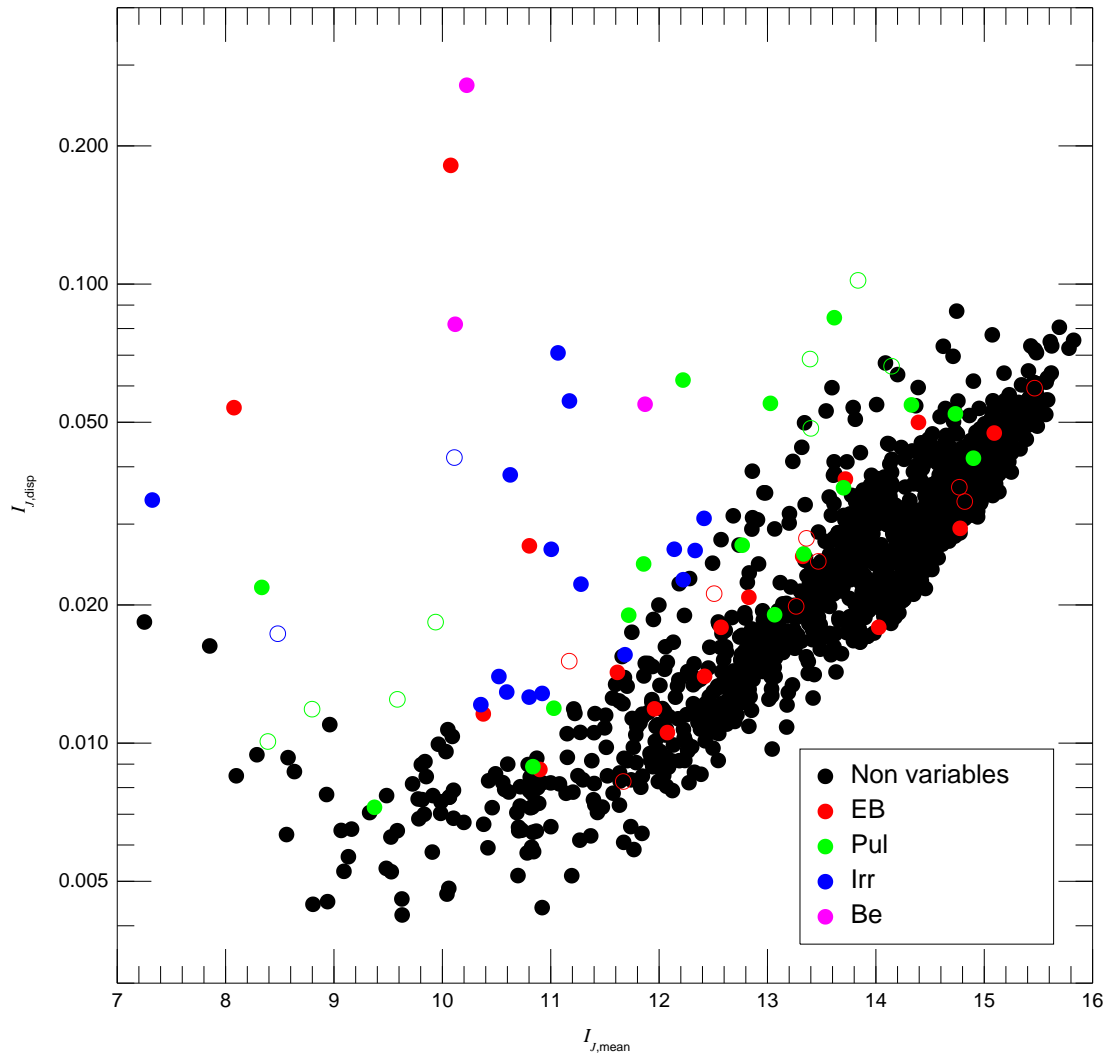


Figure 2: Dispersion - mean magnitude diagram for I_J . Non-filled symbols indicate candidate detections. The increase in dispersion in the range $I_J = 7-8$ is due to the onset on non-linearity on the CCD.

photometric calibration was performed using several reference stars by interpolating between V_J from Massey & Thompson (1991) and J from 2MASS using Maíz Apellániz (2013) and Maíz Apellániz et al. (2014). We found a photometric dispersion of 0.01 mag or less for the calibration stars.

Table 1: Confirmed and candidate eclipsing binaries.

| RA (J2000) | dec (J2000) | Names | Cand.? | R_J | I_J | Period (d) | ΔI_J |
|------------|-------------|--------------------------|--------|-------|-------|------------|--------------|
| 20:32:42.9 | 41:20:16 | ALS 21 109, [MT91] 311 | — | 13.0 | 12.0 | 6.2797(5) | 0.14 |
| 20:31:20.6 | 41:14:36 | 2MASS J20312066+4114363 | — | 13.4 | 12.1 | 8.52651(5) | 0.13 |
| 20:31:23.4 | 41:19:25 | 2MASS J20312331+4119257 | — | 16.3 | 14.8 | 7.9102(6) | 0.42 |
| 20:32:23.6 | 41:19:24 | [MT91] 242 | — | 14.8 | 14.1 | 5.6239(2) | 0.52 |
| 20:33:08.4 | 41:15:43 | [MT91] 849 | — | 16.2 | 15.1 | 2.8926(1) | 0.35 |
| 20:33:09.6 | 41:12:59 | Cyg OB2-22 C, [MT91] 421 | — | 11.7 | 10.4 | 4.1621(1) | 0.10 |
| 20:33:30.5 | 41:20:17 | V2191 Cyg, [MT91] 554 | — | 13.5 | 12.4 | 5.9504(3) | 0.28 |
| 20:31:27.8 | 41:29:17 | [MT91] 94 | — | 13.9 | 12.8 | 5.4669(5) | 0.30 |
| 20:31:41.6 | 41:28:21 | [MT91] 129 | — | 13.5 | 12.5 | 2.15175(3) | 0.07 |
| 20:33:10.5 | 41:22:22 | V2186 Cyg, [MT91] 429 | — | 12.0 | 10.9 | 2.97864(6) | 0.15 |
| 20:31:37.5 | 41:13:20 | Cyg OB2-3 A, BD +40 4212 | — | 9.2 | 8.1 | 4.74565(5) | 0.22 |
| 20:31:59.0 | 41:07:31 | 2MASS J20315898+4107314 | — | 13.0 | 11.6 | 2.53133(5) | 0.22 |
| 20:33:59.5 | 41:17:35 | Cyg OB2-27, [MT91] 696 | — | 11.2 | 10.1 | 1.46917(2) | 0.64 |
| 20:34:06.0 | 41:08:08 | ALS 15 146, [MT91] 720 | — | 12.2 | 10.8 | 4.3619(1) | 0.25 |
| 20:34:41.4 | 41:07:45 | 2MASS J20344143+4107456 | — | 14.8 | 13.3 | 2.89862(4) | 0.26 |
| 20:33:20.9 | 41:18:01 | V2189 Cyg, [MT91] 506 | — | 15.5 | 14.4 | 1.31385(5) | 0.30 |
| 20:34:45.5 | 41:14:31 | 2MASS J20344555+4114314 | — | 15.3 | 13.7 | 6.56500(5) | 0.25 |
| 20:32:38.3 | 41:28:56 | [MT91] 298 | Y | 13.4 | 12.5 | — | 0.61 |
| 20:32:34.1 | 41:22:55 | [MT91] 280 | Y | 14.4 | 13.3 | — | 0.26 |
| 20:32:11.3 | 41:25:04 | 2MASS J20321130+4125045 | Y | 16.5 | 15.5 | — | 0.60 |
| 20:32:26.8 | 41:22:35 | [MT91] 254 | Y | 15.8 | 14.8 | — | 1.42 |
| 20:32:14.0 | 41:22:24 | 2MASS J20321399+4122240 | Y | 15.8 | 14.7 | — | 1.27 |
| 20:31:57.0 | 41:12:33 | Tyc 3157-00779-1 | Y | 12.2 | 11.7 | — | 0.32 |
| 20:32:25.2 | 41:08:25 | [MT91] 245 | Y | 13.8 | 13.3 | — | 0.26 |
| 20:32:24.6 | 41:09:19 | 2MASS J20322463+4109202 | Y | 15.3 | 13.5 | — | 0.25 |
| 20:33:18.5 | 41:24:38 | 2MASS J20331846+4124383 | Y | 11.8 | 11.2 | — | 0.10 |

4 Searching for variables

In order to search for variable stars, we performed a first pass analyzing the dispersion - mean magnitude diagrams (Figure 2). In a second pass we used specific search algorithms for eclipsing binaries. For the periodogram analyses we used both the Fourier method of Horne & Baliunas (1986) and the information entropy method of Cincotta et al. (1995). We considered four types of variables:

- Eclipsing.
- Pulsating.
- Irregular/long period.
- Be stars.

For each star we assigned a detection category from non-variable, candidate, and confirmed variable. We compared our results with the previous studies of Henderson et al. (2011) and Kiminki et al. (2012).

Table 2: Confirmed and candidate pulsating variables.

| RA (J2000) | dec (J2000) | Names | Cand.? | R_J | I_J | Period (d) | ΔI_J |
|------------|-------------|-----------------------------------|--------|-------|-------|------------|--------------|
| 20:33:04.3 | 41:24:39 | [MT91] 396 | — | 14.9 | 14.3 | 1.3823(3) | 0.18 |
| 20:31:51.3 | 41:23:23 | [MT91] 152 | — | 12.3 | 11.9 | 0.99838(4) | 0.08 |
| 20:31:23.6 | 41:29:49 | 2MASS J20312356+4129489 | — | 15.7 | 14.7 | 0.9630(1) | 0.17 |
| 20:33:01.1 | 41:11:11 | [MT91] 382 | — | 14.2 | 13.7 | 0.93799(3) | 0.26 |
| 20:33:08.8 | 41:18:51 | Schulte 57 | — | 16.2 | 15.0 | 0.7275(1) | 0.17 |
| 20:33:30.8 | 41:15:22 | Cyg OB2-18, [MT91] 556 | — | 9.7 | 8.3 | 1.1192(1) | 0.07 |
| 20:34:04.0 | 41:14:43 | 2MASS J20340404+4114430 | — | 14.4 | 12.6 | 7.92(1) | 0.08 |
| 20:33:23.0 | 41:12:22 | [MT91] 514 | — | 14.4 | 13.7 | 0.84634(1) | 0.12 |
| 20:33:18.3 | 41:17:39 | V2187 Cyg, [MT91] 487 | — | 14.3 | 13.1 | 0.25385(2) | 0.06 |
| 20:33:13.3 | 41:13:28 | ALS 15 148, [MT91] 448 | — | 12.3 | 10.9 | 3.170(5) | 0.03 |
| 20:34:29.6 | 41:31:45 | ALS 15 114, [MT91] 771 | — | 10.7 | 9.4 | 1.4316(6) | 0.02 |
| 20:33:45.0 | 41:22:32 | [MT91] 626 | — | 12.2 | 11.7 | 1.11035(5) | 0.06 |
| 20:34:29.1 | 41:32:47 | 2MASS J20342909+4132476 | — | 15.5 | 12.1 | 0.9833(2) | 0.20 |
| 20:33:43.0 | 41:30:00 | 2MASS J20334299+4130005 | — | 14.2 | 13.0 | 0.95787(1) | 0.17 |
| 20:33:42.1 | 41:22:22 | [MT91] 617 | — | 14.0 | 13.3 | 1.6424(2) | 0.08 |
| 20:31:22.1 | 41:12:02 | Cyg OB2-A30 | — | 13.6 | 13.0 | 3.719(1) | 0.04 |
| 20:33:47.8 | 41:20:41 | Cyg OB2-26, [MT91] 642 | Y | 10.8 | 9.6 | — | 0.04 |
| 20:33:18.0 | 41:18:31 | Cyg OB2-8 C, [MT91] 483 | Y | 9.3 | 8.4 | — | 0.03 |
| 20:33:39.1 | 41:19:26 | Cyg OB2-19, V1393 Cyg, [MT91] 601 | Y | 10.0 | 8.2 | — | 0.04 |
| 20:35:02.5 | 41:21:27 | GSC 0316101176 | Y | 13.9 | 13.4 | — | 0.23 |
| 20:33:31.5 | 41:20:57 | [MT91] 916 | Y | 15.4 | 14.1 | — | 0.33 |
| 20:33:25.0 | 41:31:35 | Schulte 80 | Y | 14.7 | 13.4 | — | 0.16 |
| 20:33:49.8 | 41:23:58 | 2MASS J20334982+4123585 | Y | 15.1 | 13.8 | — | 0.35 |
| 20:33:39.8 | 41:22:52 | [MT91] 605 | Y | 10.9 | 9.9 | — | 0.06 |

Table 3: Confirmed and candidate irregular/long period variables.

| RA (J2000) | dec (J2000) | Names | Cand.? | R_J | I_J | Period (d) | ΔI_J |
|------------|-------------|-------------------------|--------|-------|-------|------------|--------------|
| 20:32:03.7 | 41:25:10 | [MT91] 187 | — | 12.3 | 11.3 | 222.3(3) | 0.07 |
| 20:32:14.0 | 41:23:23 | 2MASS J20321405+4123237 | — | 13.0 | 10.9 | 187.0(60) | 0.06 |
| 20:31:18.3 | 41:21:21 | ALS 15 133, [MT91] 70 | — | 11.7 | 10.3 | 192.0(40) | 0.04 |
| 20:31:39.4 | 41:21:38 | 2MASS J20313935+4121387 | — | 14.5 | 12.3 | 126.0(10) | 0.15 |
| 20:32:30.8 | 41:10:00 | Cyg OB2-B12 | — | 14.1 | 12.4 | 52.8(2) | 0.15 |
| 20:31:21.3 | 41:09:29 | 2MASS J20312131+4109286 | — | 13.0 | 12.2 | 171.0(10) | 0.08 |
| 20:33:34.3 | 41:18:11 | [MT91] 575 | — | 12.1 | 10.8 | 209.0(90) | 0.04 |
| 20:33:31.7 | 41:18:53 | [MT91] 895 | — | 14.5 | 11.7 | 34.40(3) | 0.09 |
| 20:33:25.5 | 41:20:39 | [MT91] 911 | — | 15.0 | 12.2 | 59.5(6) | 0.14 |
| 20:33:15.7 | 41:20:17 | Cyg OB2-23, [MT91] 470 | — | 11.6 | 10.6 | 192.0(90) | 0.04 |
| 20:31:36.2 | 41:22:03 | Cyg OB2-A4 | — | 13.4 | 11.0 | 96.0(10) | 0.13 |
| 20:32:32.3 | 41:27:57 | 2MASS J20323232+4127571 | — | 14.3 | 11.2 | 36.295(1) | 0.27 |
| 20:32:41.0 | 41:14:29 | Cyg OB2-12 | — | 9.5 | 7.3 | 54.0(1) | 0.18 |
| 20:33:42.1 | 41:07:53 | [MT91] 615 | — | 11.0 | 10.5 | 309.0(90) | 0.05 |
| 20:33:39.6 | 41:10:18 | 2MASS J20333961+4110192 | — | 14.4 | 11.0 | 73.5(2) | 0.33 |
| 20:33:39.5 | 41:22:36 | Cyg OB2-IRS 7 | — | 13.8 | 10.6 | 109.0(10) | 0.22 |
| 20:31:43.1 | 41:06:56 | Tyc 3157-01040-1 | Y | 10.5 | 10.1 | — | 0.18 |
| 20:33:14.8 | 41:18:42 | Cyg OB2-8 B, [MT91] 462 | Y | 9.5 | 8.5 | — | 0.11 |

Table 4: Confirmed Be stars.

| RA (J2000) | dec (J2000) | Names | Cand.? | R_J | I_J | Period (d) | ΔI_J |
|------------|-------------|-----------------------------------|--------|-------|-------|------------|--------------|
| 20:32:13.2 | 41:27:25 | Cyg OB2-4 B, [MT91] 213 | — | 11.0 | 10.8 | — | 0.70 |
| 20:33:18.5 | 41:15:35 | Schulte 64, V2188 Cyg, [MT91] 488 | — | 13.5 | 11.8 | — | 0.22 |
| 20:34:43.6 | 41:29:04 | Schulte 30, [MT91] 793 | — | 11.2 | 10.1 | — | 0.29 |

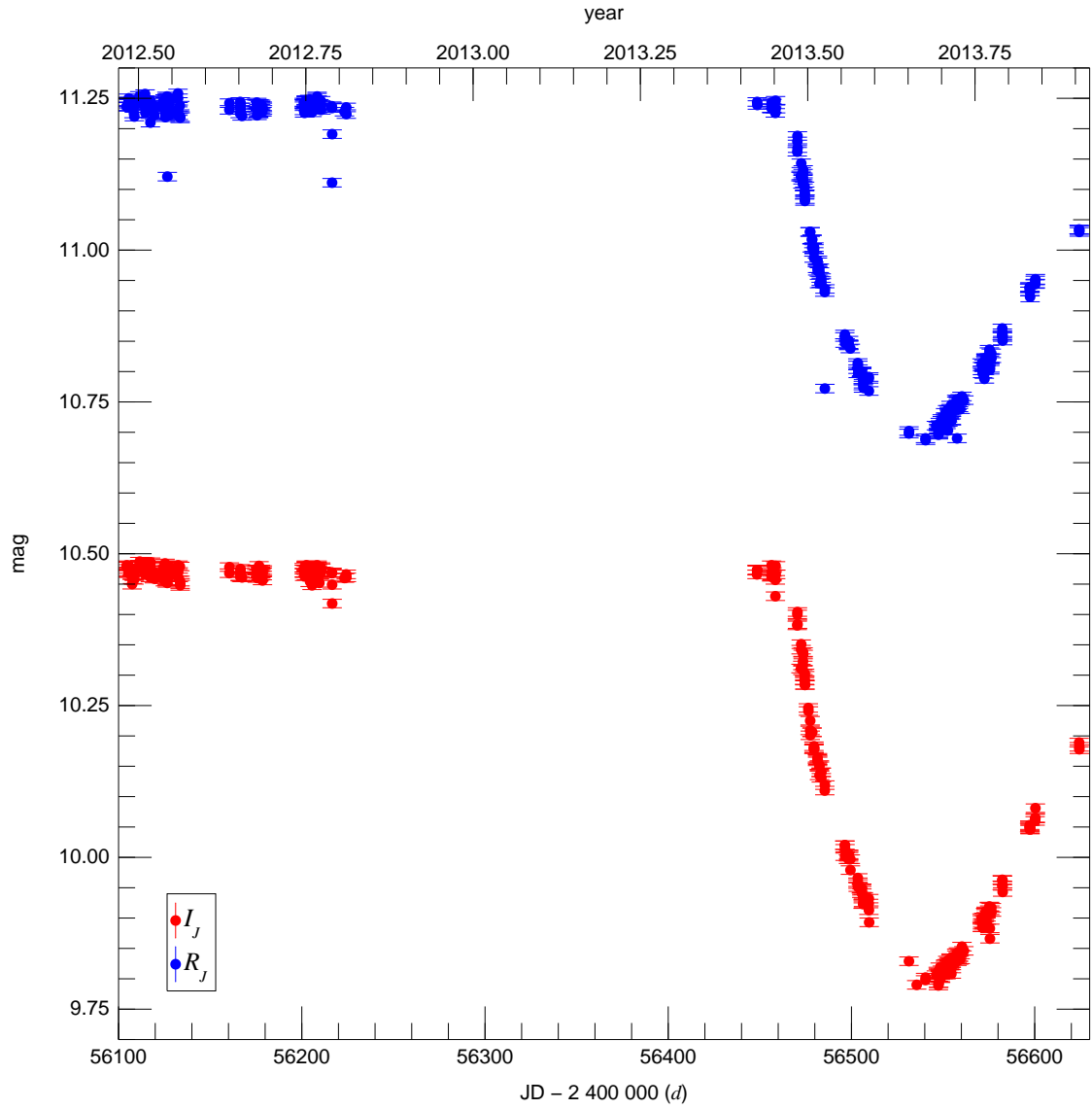


Figure 3: Light curves for Cyg OB2-4 B.

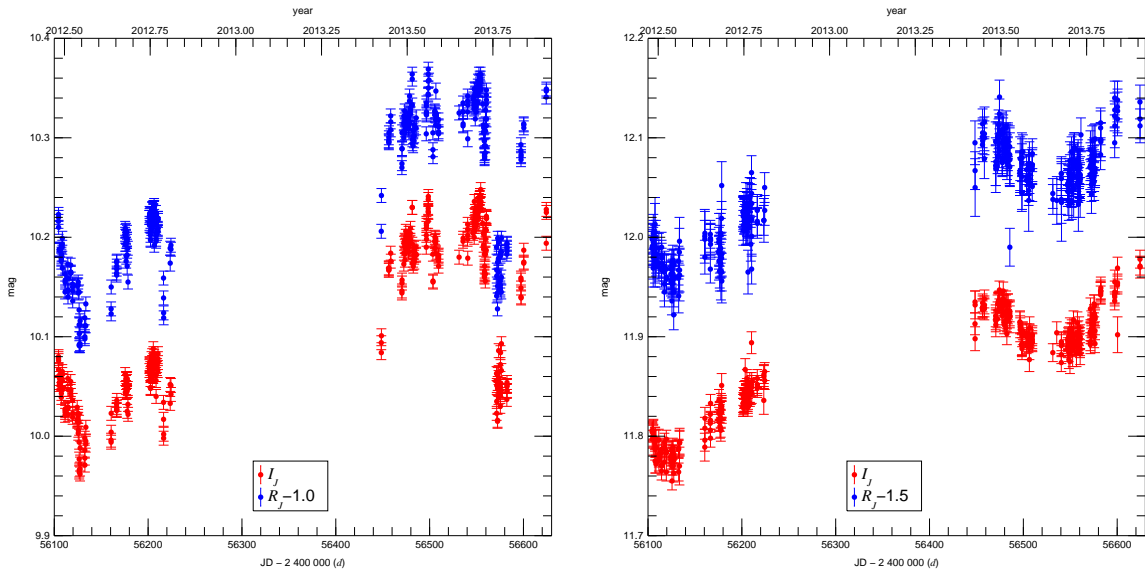


Figure 4: Light curves for two Be stars, Schulte 30 (left) and Schulte 64 (right).

5 Results

We have detected:

- 17 confirmed and 9 candidate eclipsing binaries (Table 1).
- 16 confirmed and 8 candidate pulsating variables (Table 2).
- 16 confirmed and 2 candidate irregular/long period variables (Table 3).
- 3 spectroscopically confirmed Be variable stars (Table 4).

Among the most interesting cases, we point out that Cyg OB2-4 B is a newly discovered Be star that underwent a brightening of 0.57 mag in R_J and 0.69 mag in I_J during the observing period (Salas et al. 2013, Figure 3). The event was accompanied by spectral changes e.g. H β shifted from absorption to a double-peaked emission, as seen in GOSSS data. Also, some of the eclipsing binaries have eccentric orbits (Figure 5). Finally, Cyg OB2-12 and Cyg OB2-IRS 7, two massive objects in the association, are irregular variables (Figure 8).

References

- Cincotta, P. M., Méndez, M., & Núñez, J. A. 1995, *ApJ* **449**, 231.
- Henderson, C. B. et al. 2011, *ApJS* **194**, 27.
- Horne, J. H. & Baliunas, S. L. 1986, *ApJ* **302**, 757.

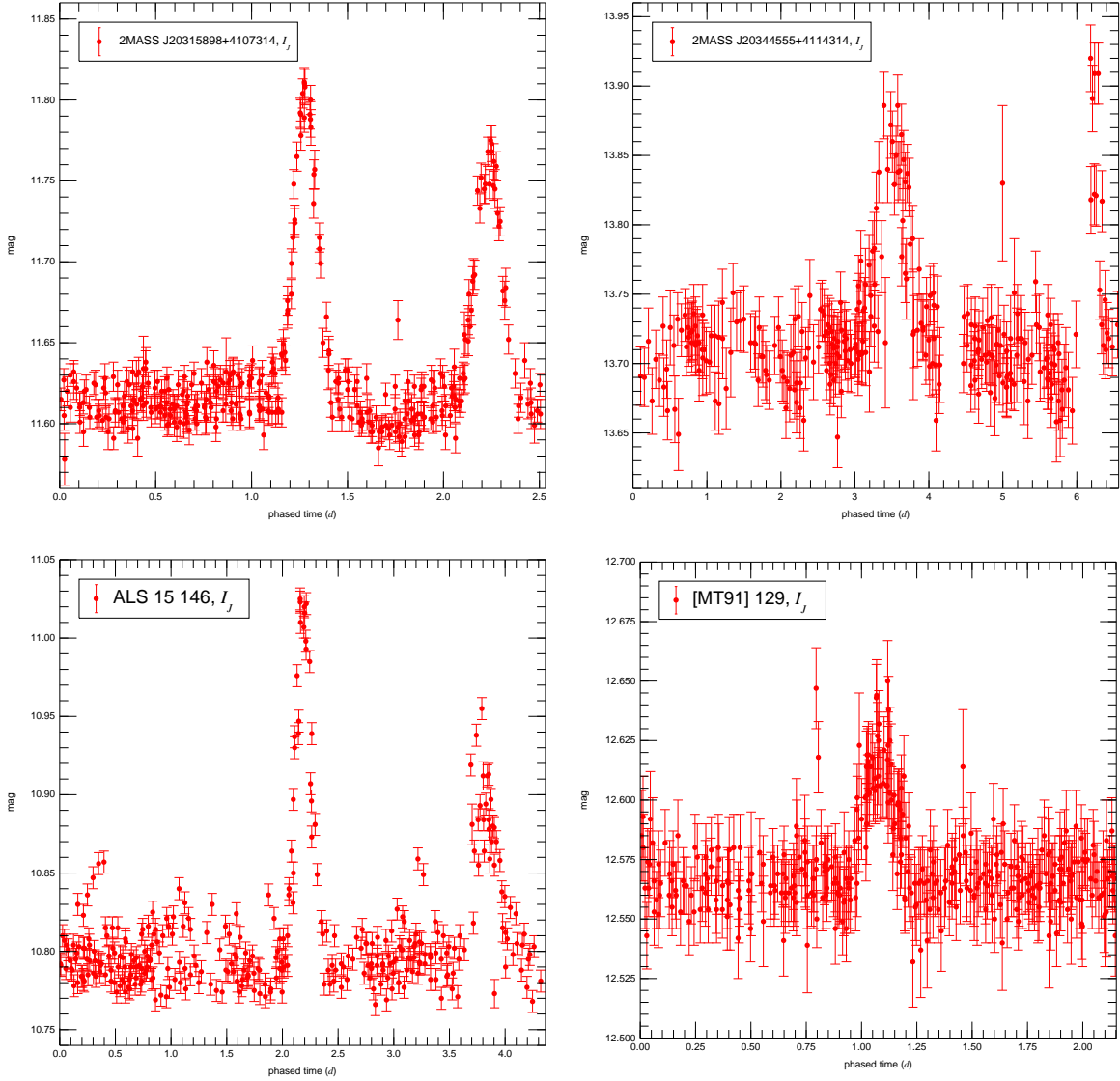


Figure 5: Phased light curves for four eclipsing binaries. Note that the first three orbits are eccentric.

- Kiminki, D. C. et al. 2012, *ApJ* **747**, 41.
- Maíz Apellániz, J. 2013, *Highlights of Spanish Astrophysics VII*, 657.
- Maíz Apellániz, J. et al. 2004, *ApJS* **151**, 103.
- Maíz Apellániz, J. et al. 2011, *Highlights of Spanish Astrophysics VI*, 467.
- Maíz Apellániz, J. et al. 2014, *A&A* **564**, A63.

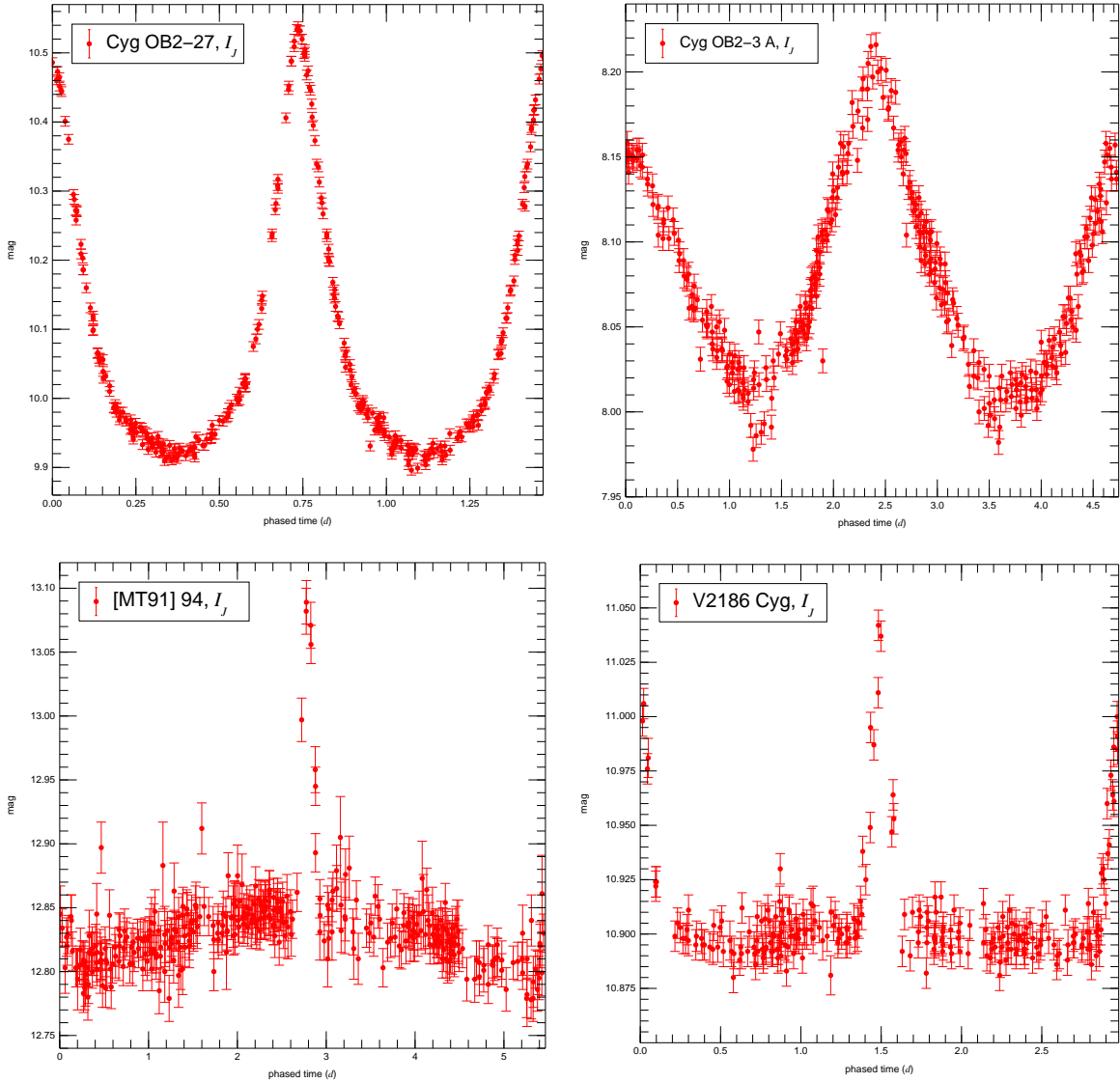


Figure 6: Phased light curves for four eclipsing binaries.

- Massey, P. & Thompson, A. B. 1991, *AJ* **101**, 1408.
- Salas, J. et al. 2013, *ATel* 5571.
- Sota, A. et al. 2008, *RvMxA&A (conf. series)* **33**, 56.
- Wright, N. J. et al. 2014, *MNRAS* **438**, 639.

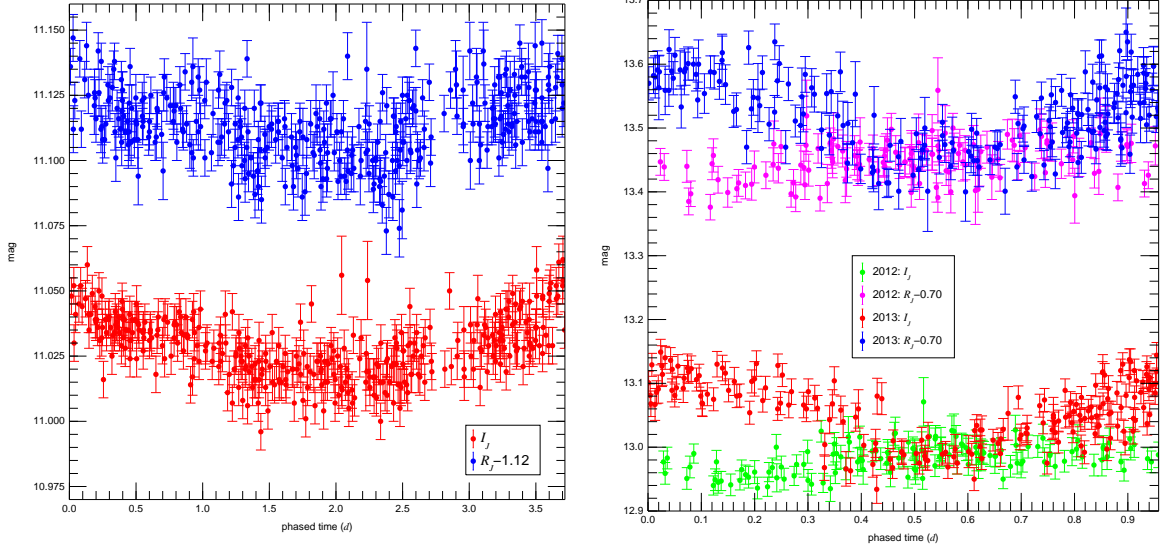


Figure 7: Phased light curves for two pulsating stars, Cyg OB2-A30 (left) and 2MASS J20334299+4130005 (right). Note how for the second case the pulsations appear only for the 2013 data.

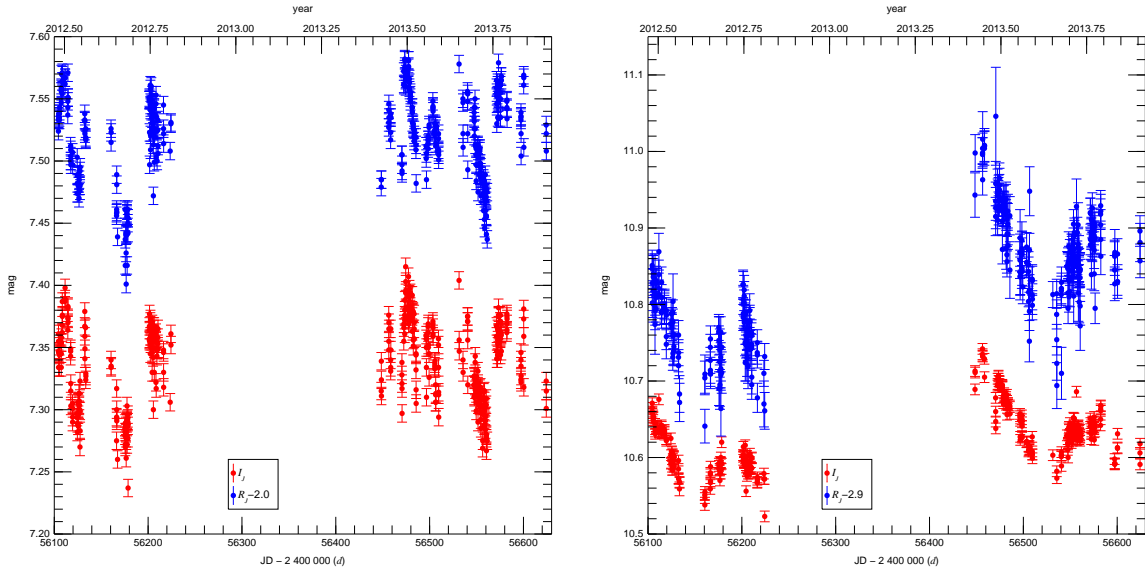


Figure 8: Light curves for two highly extinguished irregular variable stars, Cyg OB2-12 (left) and Cyg OB2-IRS 7 (right).